Pemetrexed-conjugated hyaluronan for the treatment of malignant pleural mesothelioma

Yuki Amano, Seiichi Ohta, Kazuma L. Sakura, Taichi Ito

PII: S0928-0987(19)30271-4
DOI: https://doi.org/10.1016/j.ejps.2019.105008
Article Number: 105008
Reference: PHASCI 105008

To appear in: *European Journal of Pharmaceutical Sciences*

Received date: 31 May 2019
Revised date: 4 July 2019
Accepted date: 10 July 2019

Please cite this article as: Y. Amano, S. Ohta, K.L. Sakura, et al., Pemetrexed-conjugated hyaluronan for the treatment of malignant pleural mesothelioma, European Journal of Pharmaceutical Sciences, https://doi.org/10.1016/j.ejps.2019.105008

Pemetrexed-conjugated hyaluronan for the treatment of malignant pleural mesothelioma

YUKI AMANO[A], *SEIICHI OHTA*[B], *KAZUMA L SAKURA*[C,D] *AND TAICHI ITO*[A,B] *

[A] DEPARTMENT OF CHEMICAL SYSTEM ENGINEERING, THE UNIVERSITY OF TOKYO, 7-3-1 HONGO, BUNKYO-KU, TOKYO 113-8656, JAPAN

[B] CENTER FOR DISEASE BIOLOGY AND INTEGRATIVE MEDICINE, THE UNIVERSITY OF TOKYO, 7-3-1 HONGO, BUNKYO-KU, TOKYO 113-0033, JAPAN

[C] RESPIRATORY CENTER, OSAKA UNIVERSITY HOSPITAL, SUITA, OSAKA, 565-0871, JAPAN

[D] DEPARTMENT OF SURGERY, OSAKA UNIVERSITY, SUITA, OSAKA, 565-0871, JAPAN

* CORRESPONDING AUTHOR.

CENTER FOR DISEASE BIOLOGY AND INTEGRATIVE MEDICINE, THE UNIVERSITY OF TOKYO, 7-3-1 HONGO, BUNKYO-KU, TOKYO 113-8655, JAPAN

TEL: +81-3-5841-1696; FAX: +81-3-5841-1697

E-mail address: taichi@m.u-tokyo.ac.jp

Abstract: Pemetrexed (PMX) is a multi-targeted antifolate drug used for the treatment of malignant pleural mesothelioma (MPM) and non-small cell lung cancer. Hyaluronan (HA) in blood is well known as a disease marker of MPM. We synthesized PMX-conjugated hyaluronan (HA-ADH-PMX) for the first time to develop a novel anticancer chemotherapeutic agent. HAs with different molecular weights (76 and 130 kDa) were first derivatized with adipic dihydrazide (ADH) and then conjugated to PMX. The obtained HA-ADH-PMX retained inhibitory activity against folate metabolism enzymes; thymidylate synthase was inhibited to the same extent as native PMX, whereas the inhibition constant against dihydrofolate reductase was 3.3% for 76 kDa HA-ADH-PMX and 12% for 130 kDa HA-ADH-PMX when compared with that of native PMX. The *in vitro* cytotoxicity of HA-ADH-PMX from both molecular weights against MPM cell lines was lower than that of native PMX. On the other hand, intrapleural administration of 76 kDa HA-ADH-PMX resulted in a survival rate of MPM model mice comparable to that with native PMX, suggesting the potential for future MPM therapy.

***Keywords*:**

Anti-tumor, Drug conjugates, Pemetrexed, Malignant pleural mesothelioma

1. Introduction

Pemetrexed (PMX) is a multitargeted antifolate for cancer treatment. PMX inhibits multiple enzymes involved in folate metabolism, such as thymidylate synthase (TS), dihydrofolate reductase (DHFR) and glycinamide ribonucleotide formyltransferase (GARFT), leading to the interference of DNA synthesis (Hanauske, et al., 2001; Schultz, 2005). PMX is a relatively new antifolate compared with other drugs such as methotrexate (MTX), whose polymer conjugation has actively been investigated for long time (Boratyński, et al., 2000; Chau, et al., 2004; Homma, et al., 2009; Shin, et al., 2014). PMX was approved by FDA in 2004 for treatment of malignant pleural mesothelioma (MPM), and now also be used for non-small cell lung cancer (Genova, et al., 2013).

Malignant pleural mesothelioma (MPM) is an aggressive mesothelial tumor of pleura that caused by asbestos exposure (Thompson, et al., 2014). MPM has a long latency period of about 40-50 years, therefore it is predicted that patient number will acceleratively increase in near future. For the therapeutic treatment of MPM, a combination therapy of intravenous administration of pemetrexed (PMX) and cisplatin (CDDP) is currently the clinical standard (Baas, 2007). However, five-year survival rate of MPM patients is less than 10 % and the standard therapy causes strong side effects. Nivolumab was approved in 2018 in Japan for advanced/recurrent MPM which became unresectable after the standard therapy (Fujimoto, et al., 2018). However, there is a risk of immune-mediated adverse reactions. Therefore, new therapeutic strategies which show high

THERAPEUTIC EFFECT AND LOW SIDE EFFECT TO TREAT MPM ARE STILL IN HIGH DEMAND.

Conjugation of PMX to polymers, as well as its loading to drug carriers, can be a promising approach to improve its therapeutic efficacy. This strategy is expected to improve the poor water solubility and short retention time, which are main drawbacks of PMX. The synthesis of two polymer conjugates have been reported so far; POLYETHYLENE GLYCOL (PEG) (VANDANA AND SAHOO, 2012), AND hydroxyethyl starch (HES) (CIEKOT, ET AL., 2016). IN THE CASE OF PMX-CONJUGATED PEG, COMPARABLE CELL CYTOTOXICITY AND LONGER RETENTION TIME THAN NATIVE PMX WAS REPORTED (VANDANA AND SAHOO, 2012), ALTHOUGH ITS THERAPEUTIC EFFECT *IN VIVO* IS NOT REPORTED YET. IN THE CASE OF PMX-CONJUGATED HES, ITS THERAPEUTIC EFFECT WAS NOT STUDIED BOTH *IN VITRO* AND *IN VIVO* (CIEKOT, ET AL., 2016). THUS, FURTHER INVESTIGATION ON POLYMER CONJUGATION IS EXPECTED FOR PMX.

HYALURONAN (HA) IS a glycosaminoglycan that is one of the major components of extra cellular matrix. It is well known that HA in pleural effusion is utilized clinically as a prognostic marker in MPM (LOURDES AND RALPH, 2017; CREANEY, ET AL., 2013). The viscosity of the plural effusion is extremely high in some patients of MPM due to its high concentration of HA. Thus, it is speculated that the turnover of HA would be relatively active compared to normal tissues (LI AND HELDIN, 2001). Generally speaking, HA is internalized by cells via binding to its receptors such as CD44 and subsequently inducing receptor-mediated endocytosis in its turnovers process both in normal tissues and cancer tissues (CICHY AND PURE, 2003; MISRA, ET AL., 2015). Because CD44 is overexpressed in tumor cells with high affinity state, it is expected that HA is aggressively taken up and then metabolized via this transport pathway in cancer cells. By taking advantage of these characteristic interactions with

tumors, HA has been studied as a targeted drug carrier for wide range of cancers (Luo, et al., 2002; Cai, et al., 2010; Ohta, et al., 2016; Ohta, et al., 2017; Luo and Prestwich, 1999; Lee, et al., 2008; Oommen, et al., 2014).

Here, we developed a novel HA-based PMX conjugate (HA-ADH-PMX), aiming to render cancer-targeting ability via active HA turn over, as well as improved water solubility and prolonged residence time (Figure 1A). HA with different molecular weights were first derivatized with adipic dihydrazide (ADH), and then conjugated to PMX. Their effect on enzyme inhibition activity, cellular internalization, and growth inhibition against MPM cell lines were examined *in vitro*. Their anti-tumor activity was also evaluated using a mouse model of MPM.

2. Materials and method

2.1. Materials

HA was kindly gifted from Denka Co. (Tokyo, Japan). ADH, *N*-hydroxysuccinimide (NHS), dicyclohexylcarbodiimide (DCC), insulin, Roswell Park Memorial Institute media (RPMI-1640), penicillin-streptomycin-amphotericin B (PSA), MEM Non-essential Amino Acids Solution (× 100) (NEAA), sodium pyruvate, 2-Mercaptoehanol were purchased from Wako Pure Chemical Industries (Osaka, Japan). 1-Ethyl-3-(3-(dimethylamino)propyl) carbodiimide hydrochloride was purchased from Peptide Institute, Inc. (Osaka, Japan). 1-Hydroxybenzotriazole Monohydrate (HOBt), pemetrexed Hydrate (PMX) were purchased from Tokyo Chemical Industry (Tokyo, Japan). 2-[4-(2-Hydroxyethyl)-1-piperazinyl] ethanesulfonic acid (HEPES) was purchased from Dojindo

LABORATORIES (KUMAMOTO, JAPAN). Dihydrofolate Reductase Assay Kit was purchased from SIGMA–ALDRICH (ST. LOUIS, MO, USA). MEDIUM 199 WAS THERMO FISHER SCIENTIFIC INC. (WALTHAM, MA, USA). HYDROCORTISONE WAS PURCHASED FROM MP BIOMEDICALS (SANTA ANA, CA, USA). Fetal bovine serum was purchased from Biosera, Inc., (Villebon sur Yvette, France), and epidermal growth factor was purchased from PeproTech Ltd. (London, UK). Dialysis membrane (Spectra/Por, MWCO = 6000–8000 Da) was purchased from Spectrum Laboratories Inc. (Rancho Dominguez, CA, USA). The human pleural mesothelial cell line, MeT-5A, was purchased from American Type Culture Collection (Rockville, MD, USA). Recombinant Human Thymidylate Synthase protein (ab95378) was purchased from Abcam (Cambridge, UK).

2.2. CONJUGATION OF ADIPIC DIHYDRAZIDE TO HA (HA-ADH)

HA-adipic dihydrazide (HA-ADH) was synthesized as described previously (EMOTO, ET AL., 2014; YEO, ET AL., 2006; BULPITT AND AESCHLIMANN, 1999). IN BRIEF, 1.5 G OF HA (MW = 65, 130, 850 KDA) WAS DISSOLVED IN 300 ML OF DISTILLED WATER, TO WHICH 16.3 G OF ADH WAS ADDED. THEN HOBT (2.28 G IN 15 ML OF DMSO) AND EDC· HCL (3.24 G IN 9 ML OF DISTILLED WATER) WERE ADDED DROPWISE TO THE MIXTURE. THE PH WAS ADJUSTED TO 5.5 WITH 1 M HCL OR 1 M NAOH AND KEPT CONSTANT FOR 4 H. THE REACTION WAS ALLOWED TO PROCEED OVERNIGHT. THE SOLUTION WAS DIALYZED AGAINST DISTILLED WATER FOR 6 DAYS AND THEN LYOPHILIZED.

2.3. SYNTHESIS OF NHS ESTER LABELING PEMETREXED

THE CARBOXYLATE GROUP OF PEMETREXED WAS ACTIVATED USING NHS AND DCC AS DESCRIBED PREVIOUSLY (VANDANA AND SAHOO, 2012).

Briefly, 0.4 g of pemetrexed hydrate was dissolved in 8 mL of super-dehydrated DMSO and then reacted with 0.12 g of NHS and 0.21 g of DCC in darkness at room temperature for overnight. Then, the insoluble byproduct, dicyclohexylurea was removed by filtration. The obtained DMSO solution of NHS-PMX was stored at -20 °C until use in further synthesis.

2.4. Synthesis of HA-ADH-PMX

HA-ADH-PMX was synthesized by reacting HA-ADH with 2 molar equivalents of NHS-PMX to ADH. The activated PMX was reacted with 0.2 g of HA-ADH dissolved in 26.66 mL of 0.1 M $NaHCO_3$ solution at room temperature for 18 h. The resultant solution was dialyzed against distilled water for 3 days and then lyophilized.

2.5. Synthesis of HA-ADH-RITC-PMX

Rhodamine-conjugated HA-ADH (HA-ADH-RITC) was synthesized by reacting HA-ADH with 0.04 molar equivalents of rhodamine B isothiocyanate (RITC) as shown in Figure S1. 0.5 g of HA-ADH was dissolved in 100 mL of distilled water, to which RITC (9.5 mg in 3.5 mL of DMSO) were added dropwise. The reaction was allowed to proceed overnight in darkness at room temperature. After that, the solution was dialyzed against distilled water for 3 days and then lyophilized. HA-ADH-RITC-PMX was synthesized by reacting HA-ADH-RITC with NHS-PMX in the same way as HA-ADH-PMX.

2.6. Characterization of HA-ADH-PMX

Synthesis of HA-ADH-PMX was confirmed by ^{1}H NMR (αJEOL JNM-A500, JEOL), FT-IR (FT/IR-4200ST, JASCO) and UV-vis (V-630BIO, JASCO). The polymers were dissolved in D_2O and PMX was dissolved in DMSO-d6 for ^{1}H NMR analysis. FT-IR spectra were measured using a potassium bromide (KBr) tablet of each polymer. UV-vis absorption spectra of polymers were measured in phosphate buffer saline (pH 7.4). The absolute molecular weight and root-mean-square radius were determined by SEC-MALS (DAWN8^{+}, Wyatt Technology Corp.). Separation was performed at room temperature using Shodex OHpak LB-806M column (Showa Denko Co., Ltd.) at a flow rate of 0.5 mL/min. Sodium phosphate buffer (pH 6.7), composed of 0.05 M phosphate buffer containing 0.2 M NaCl was used as a mobile phase. Mw and radius values were calculated by Astra v7.1 software, using a dn/dc value of 0.153 (Weigel and Baggenstoss, 2017).

2.7. Cell-free assay of thymidylate synthase (TS) activity

TS activity was measured spectrophotometrically as previously described (El-Naggar, et al., 2017; Wahba and Friedkin, 1962). TS irreversibly converts tetrahydrofolate (THF) and deoxyuridine monophosphate (dUMP) to DHF and deoxythymidine monophosphate (dTMP). This reaction can be monitored by the absorbance change at 340 nm, which corresponds to the DHF formation. The assay was conducted in assay buffer at pH 7.4 which contains 100 mM of 2-mercaptoethanol, 20 mM of $MgCl_2$, 12 mM of formaldehyde, 40 mM of TrisHCl, and 0.75 mM of NaEDTA (Solution A). THF was dissolved in solution A at 1.1 mM (Solution B). PMX and HA-ADH-PMX were dissolved in

solution A equivalent to 1 mM of PMX (Solution C). dUMP was dissolved in solution A at 100 mM (Solution D). 333µL of solution A, 135 µL of solution B, 25 µL of solution C and 5 µL of solution D were added in a microtube and mixed gently, then transferred to a micro-cuvette. Finally, 2 µL of TS was added and gently shaken. Then absorbance at 340 nm was continuously measured for 10 min. TS activity was determined by the amount of absorbance change after 10 min at 37 °C.

2.8. Cell-free assay of dihydrofolate reductase (DHFR) activity

DHFR activity was measured with a DHFR assay kit (Sigma-aldrich) spectrophotometrically as previously described (Kao, et al., 2008; Stone and Morrison, 1986; Navarro-Perán, et al., 2005). DHFR irreversibly converts DHF and NADPH to THF and $NADP^+$. The rate of THF formation can be continuously monitored by the absorbance change at 340 nm, which corresponds to the conversion of DHF and NADPH. PMX and HA-ADH-PMX were dissolved in the assay buffer 10× equivalent to 10 mM of PMX (Solution A). NADPH was dissolved in the assay buffer 0.2× at 10 mM (Solution B). DHF was dissolved in the assay buffer 10× at 10 mM (Solution C). 464.5 µL of the assay buffer 1×, 25 µL of DHFR and 5 µL of solution A were added in microtube and mixed gently, then transferred to a micro-cuvette. 3 µL of solution B was added in this cuvette and gently shaken. Finally, 2.5 µL of solution C was added and gently shaken. Then absorbance change at 340 nm was

continuously measured for 10 min. DHFR activity was determined by the amount of absorbance change after 10 min at 37 °C.

2.9. Determination of inhibition constant of DHFR

PMX and HA-ADH-PMX were dissolved in the assay buffer 10× equivalent to 100 μM of PMX (Solution A). NADPH was dissolved in the assay buffer 0.2× at 10 mM (Solution B). DHF was dissolved in the assay buffer 10× at 312.5 μM - 10 mM (Solution C). 487 μL of the assay buffer 1×, 2.5 μL of DHFR and 5 μL of solution A were added in microtube and mixed gently, then transferred to a micro-cuvette. 3 μL of solution B was added in this cuvette and gently shaken. Finally, 2.5 μL of solution C was added and gently shaken. Then absorbance change at 340 nm was continuously measured. Inhibition of initial velocity was determined by the absorbance change for 1.5 min. The plot of initial velocity of absorbance change as a function of DHF concentration was used for determination of inhibition constant.

2.10. Cell culture

MSTO-211H human malignant pleural mesothelioma cells and AB22 mouse malignant pleural mesothelioma cells were grown in RPMI-1640, which contained 10 mM HEPES, 10 % fetal bovine serum, 1 mM sodium pyruvate, 100 μM non-essential amino acids, 50 μM 2-mercaptoethanol and 1 % penicillin-streptomycin-amphotericin B. MeT-5A human normal mesothelial cells were grown in Medium 199,

which contained 25 mM HEPES, 10 % fetal bovine serum, 3.3 nM epidermal growth factor, 400 nM hydrocortisone, and 870 nM insulin.

2.11. Cellular uptake of HA-ADH-PMX

The cells were seeded on a 60-mm dish with an initial density of 0.8×10^5 cells/dish and incubated at 37 °C in 5 % CO_2 for 2 days. The growth medium was replaced with growth medium containing 0.1 mg/mL of rhodamine labeled HA-ADH-PMX. The cells were incubated for 6 h at 37 °C. After the incubation, the cells were washed with PBS then analyzed by fluorescent microscope (BZ-X810, Keyence). Then cells were trypsinized and collected. Finally, cells were resuspended in PBS (5×10^5 cells/mL) and transferred to sample tubes. Each sample was analyzed using a flow cytometer (BD LSR2; BD Biosciences) equipped with 488 nm laser. A total of 10000 events were recorded for each measurement. We normalized the fluorescent intensity measured by flow cytometry by considering the difference of rhodamine modification degree in HA-ADH-PMX to evaluate the amount of cellular uptake.

2.12. Dose dependent cytotoxicity of HA-ADH-PMX

Anti-cancer activity of HA-ADH-PMX was evaluated with the WST-8 assay (Cell Counting Kit-8; Dojindo Laboratories) using MSTO-211H, AB22 and MeT-5A cells. The cells were seeded on a 24-well plate with an initial density of 50000 cells/well and incubated at 37 °C in 5 % CO_2 overnight. Then cells were treated

with PMX and HA-ADH-PMXs equivalent to 10^{-4} to 10^{2} μg/mL of PMX. After 48 h, 50 μL of tetrazolium salt solution (WST-8) was added to each well and incubated at 37 °C for 1 h. The absorbance at 450 nm was measured using a plate reader (2030 ARVO V3; PerkinElmer, Waltham, MA, USA). The absorbance value of each well was normalized by that of control wells in which no drugs were added to the media.

2.13. Time dependent cytotoxicity of HA-ADH-PMX

The cells were seeded on a 24-well plate with an initial density of 50000 cells/well and incubated at 37 °C in 5 % CO_2 overnight. Then cells were treated with HA-ADH-PMX equivalent to 10 μg/mL of PMX. After 1, 3, 6, 10 h, the cells were washed with PBS and then fresh culture media were added. The cells were incubated for another 24 h, then 50 μL of tetrazolium salt solution (WST-8) was added to each well and incubated at 37 °C for 1 h. The absorbance at 450 nm was measured using plate reader. The absorbance value of each well was normalized with that of control wells in which no drugs were added to the media.

2.14. Evaluation of antitumor activity in mouse models of MPM

These experiments were performed at the Animal Research Section, Center for Disease Biology and Integrative Medicine, Faculty of Medicine, The University of Tokyo. The Animal Care Committee of the University of Tokyo approved all of the procedures performed in this study before it began.

BALB/cAJcl mice (9 weeks old, female) weighing 21-26 g were purchased from CLEA Japan, Inc. All the animals were in quarantine for 1 week prior to the experiment. HA-ADH-PMX was sterilized by ethylene oxide.

Mouse model of MPM was prepared as previously described (Sasai, et al., 2016). AB22 cells were trypsinized and collected from culture dishes. 2×10^5 cells of AB22 were resuspended in 100 μL of PBS, to which 50 μL of Matrigel was added. Then 150 μL of cell suspension was injected into the right pleural cavity of mice under general anesthesia with a 100 μL of mixture agent (4 mg/kg of midazolam, 5 mg/kg of butorphanol tartrate and 0.75 mg/kg of medeto-midine). 7 days after the cell implantation, PMX and HA-ADH-PMX dissolved in saline were injected into the right pleural cavity at 60 mg/kg-PMX under the same anesthesia condition as described above. To evaluate the anti-tumor effect of HA-ADH-PMXs, survival time of the mice was recorded. Differences between groups in the survival experiment were determined using Kaplan-Meier log-rank test. A *P*-value less than 0.05 was considered as statistically significant.

3. Results and Discussion

3.1. Synthesis and characterization of HA-ADH-PMX

Synthetic route of HA-ADH-PMX is shown in Figure 1B. Briefly, HA with different molecular weights were conjugated with ADH at a first step of the synthesis, as described in previous reports (Emoto, et al., 2014; Yeo, et al., 2006; Bulpitt and Aeschlimann, 1999).

HA-ADH-PMX was then synthesized by reacting HA-ADH with *N*-hydroxysuccinimide-activated PMX (NHS-PMX).

Synthesis of HA-ADH was confirmed by using ^{1}H NMR and FT-IR. In the ^{1}H NMR spectra, methylene proton of conjugated ADH was confirmed at 1.5 ppm (Figure 2A). We determined the degree of ADH modification by using this peak. The degree of ADH modification to HA was 0.413 to its disaccharide unit of HA. In the FT-IR spectra, HA-ADH exhibited its characteristic peaks at 1648 cm^{-1} due to amide I band (Figure 2B).

Synthesis of HA-ADH-PMX was confirmed by using ^{1}H NMR, FT-IR and UV-vis. In the ^{1}H NMR spectra, the aryl proton of conjugated PMX (singlet peaks at 7.2 and 7.7 ppm) was confirmed after the PMX modification (Figure 2A). As shown in Figure 2B, HA-ADH-PMX generated its characteristic peak at 2860 cm^{-1} due to symmetric stretch vibration of methylene protons of PMX. As shown in Figure 2C, PMX had an absorption peak in the range of wavelength between 220-320 nm, while HA did not. In the spectrum of HA-ADH-PMX, an absorption peak was emerged in the same range as PMX. The degree of PMX modification was calculated from its absorbance at 225 nm, which is a representative peak of PMX. The degree of PMX modification was 0.262 to its disaccharide unit of HA. The spectra of ^{1}H NMR, FT-IR and UV-vis of HA-ADH-PMX from 130 kDa and 850 kDa showed similar results of those from 65 kDa, which are shown in Figure S2 and S3, respectively. These results suggested that PMX was successfully conjugated to HA.

Solubility of HA-ADH-PMXs depended on their molecular weight to a great extent. HA-ADH-PMXs were dissolved in phosphate buffer saline (PBS) at 0.1 % (Figure 3A). Whereas HA-ADH-PMX from 65 kDa and 130 kDa were completely dissolved in PBS, that from 850 kDa HA was only swelled, and thus undissolved solids were present even after overnight stirring. Because of this insolubility, HA-ADH-PMX from HA with 850 kDa was not investigated any more in this research. Therefore, we only used HA-ADH-PMX from 65 kDa and 130 kDa HA for further investigations.

Size of HA-ADH-PMX is important to determine its endocytosis efficiency. We then measured the absolute molecular weight and root-mean-square radius of HA-ADH-PMX by size exclusion chromatography coupled to multiangle light scattering (SEC-MALS). Figure 3B shows elution curve of polymers. The resulting weight-average molecular weight of HA-ADH-PMXs synthesized from 65 kDa and 130 kDa HA were 76 kDa and 130 kDa, respectively, suggesting the negligible effect of the conjugation reactions on the molecular weight. On the other hand, decrease of molecular size was observed by the conjugation of PMX. Whereas the molecular sizes of HA with 65 kDa before the conjugation measured by MALS were 39 nm, those after the conjugation were 28 nm. In the same way, the molecular sizes of HA with 130 kDa before the conjugation measured by MALS were 60 nm, whereas those after the conjugation were 40 nm. It was considered that the conjugation of PMX increased hydrophobicity of the polymer, which induced the polymer shrinking. Decrease of

POLYMER HYDRODYNAMIC SIZE BY CONJUGATION OF HYDROPHOBIC MOLECULES WAS ALSO REPORTED IN PREVIOUS WORKS (PRAVATA, ET AL., 2008; HARDING, 1997). WE NAMED HA-ADH-PMX WITH DIFFERENT MOLECULAR WEIGHT AS HA-ADH-PMX (76 KDA) AND HA-ADH-PMX (130 KDA) HEREAFTER. RESULTS OF THESE CHARACTERIZATIONS WERE SUMMARIZED IN TABLE 1. THESE RESULTS SUGGESTED THAT THE SIZES OF HA-ADH-PMXS MIGHT BE SUITABLE FOR ENDOCYTOSIS.

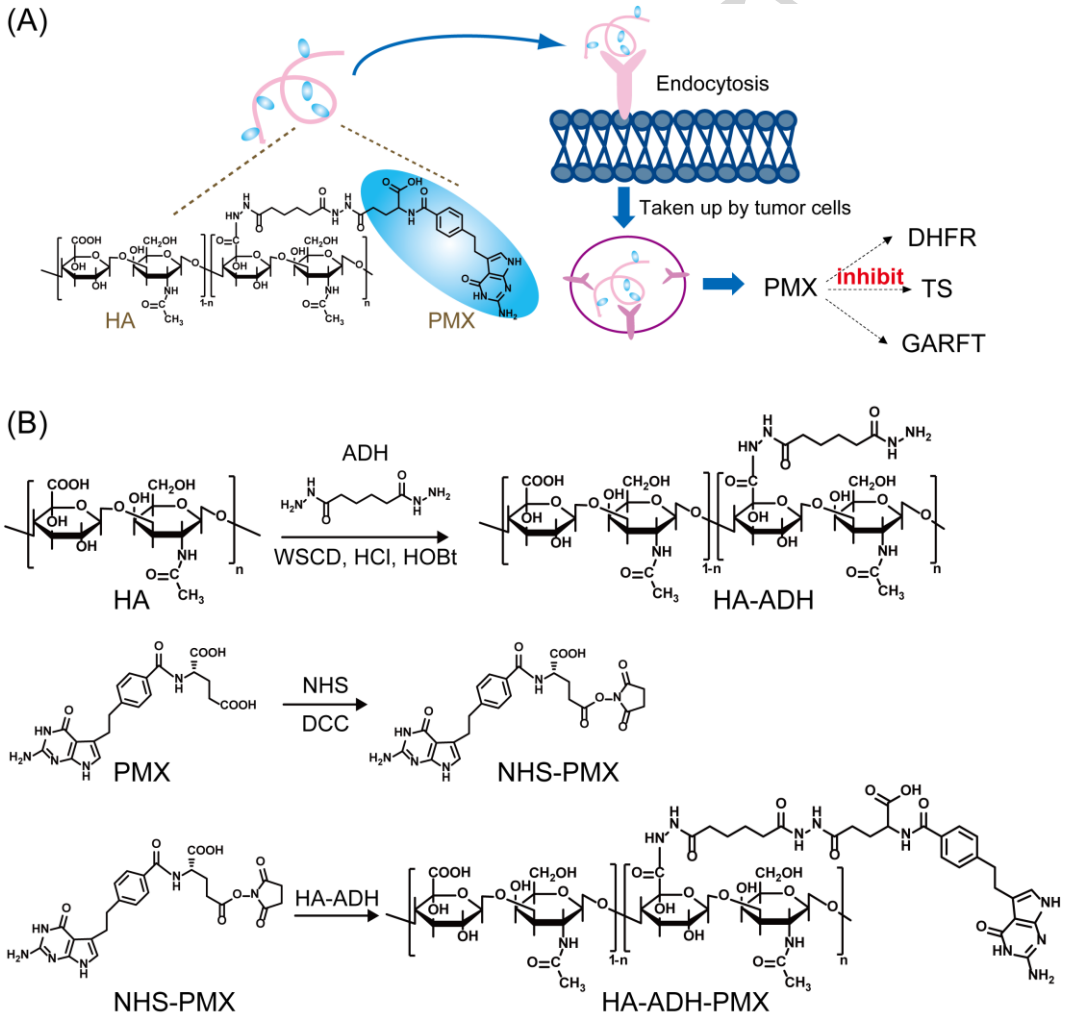

FIGURE 1. (A) SCHEMATIC ILLUSTRATION FOR THE CONCEPT OF THIS RESEARCH. (B) SYNTHETIC ROUTE OF PMX-CONJUGATED HA (HA-ADH-PMX).

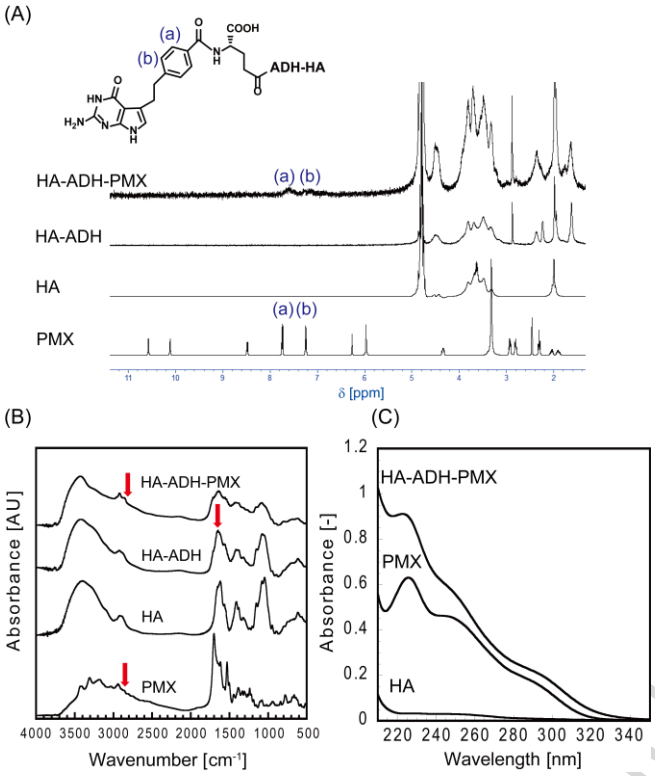

FIGURE 2. (A) ^{1}H NMR SPECTRA OF PMX IN DMSO-D6, HA IN D_2O, HA-ADH IN D_2O, AND HA-ADH-PMX IN D_2O. (B) FT-IR SPECTRA OF PMX, HA, HA-ADH AND HA-ADH-PMX. ARROWS INDICATE THE CHARACTERISTIC PEAKS AT 2860 CM^{-1} AND 1648 CM^{-1}. (C) UV-VIS SPECTRA OF PMX, HA, AND HA-ADH-PMX IN PBS.

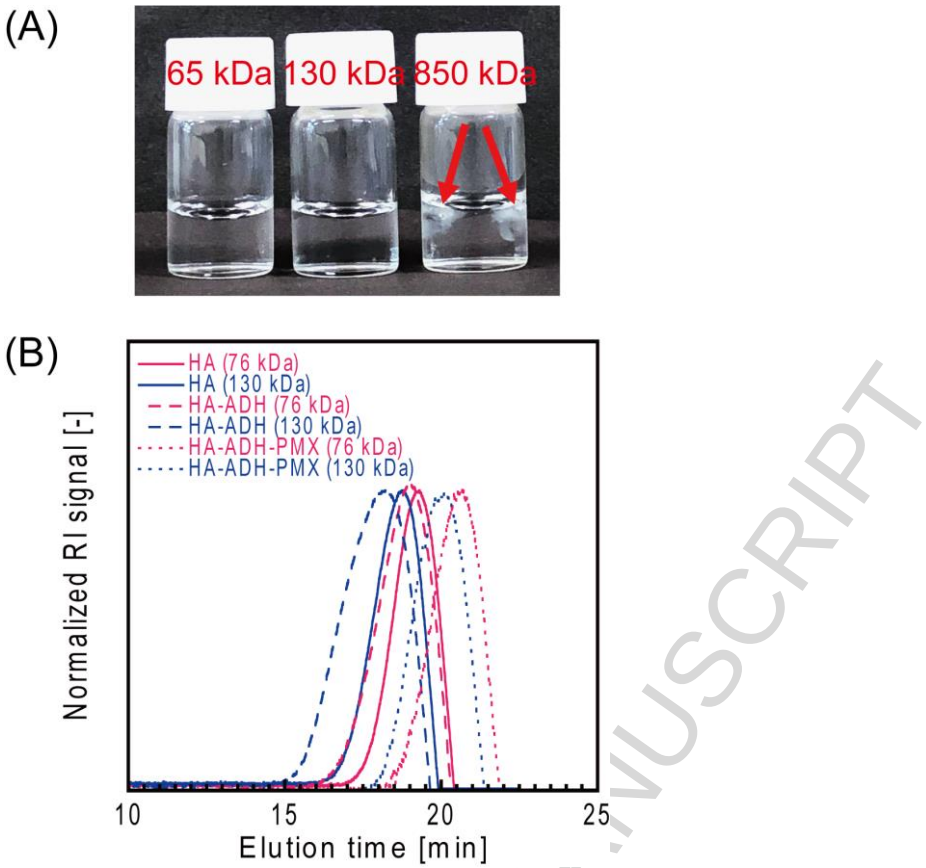

FIGURE 3. (A) IMAGES OF DIFFERENT MOLECULAR WEIGHTS OF HA-ADH-PMX DISSOLVED IN PBS. HA-ADH-PMX SYNTHESIZED FROM 65 KDA AND 130 KDA HA WERE COMPLETELY DISSOLVED, WHILE THAT FROM 850 KDA WAS NOT. (B) ELUTION CURVES OF HA, HA-ADH AND HA-ADH-PMX MEASURED BY GPC.

TABLE 1. SUMMARY OF THE CHARACTERIZATION OF HA-ADH-PMX

MW OF HA [KDA]	ADH [MOL/MOL-HA]	PMX [MOL/MOL-HA]	MW OF HA-ADH-PMX [KDA]	SIZE [NM]
65	0.41	0.26	76	28
130	0.43	0.22	130	40

3.2. INHIBITORY ACTIVITIES OF HA-ADH-PMXS AGAINST TS AND DHFR

Pharmacological effects of HA-ADH-PMXs would relate to the conjugate site of PMX and molecular weight of HA backbone. Main folate metabolism enzymes were evaluated spectrophotometrically as previously described (El-Naggar, et al., 2017; Wahba and Friedkin, 1962; Kao, et al., 2008; Stone and Morrison, 1986; Navarro-Perán, et al., 2005). THF and DHF, which are substrate for TS and DHFR respectively, were incubated with these enzymes under the existence of HA-ADH-PMX or native PMX. Figure 4A shows the inhibitory activity of HA-ADH-PMX against TS. After 10 min of incubation, the addition of HA-ADH-PMX (76 kDa) and HA-ADH-PMX (130 kDa) significantly decreased the absorbance change to 59 % and 56 % of the control without inhibitors, which was almost the same level with native PMX (55% decrease compared with the control). These results indicated that HA-ADH-PMXs retained TS inhibitory activities as high as native PMX, even after the conjugation. It has been reported that TS inhibitors, including PMX, bind to TS through two essential moieties: pyrimidine and glutamate (El-Naggar, et al., 2017). Pyrimidine moiety binds to pyrimidine-binding site of the enzyme, while glutamate moiety binds to its folate-binding site. Although HA-ADH-PMX does not preserve the bindable domain to folate-binding site because of the conjugation through carboxylate group of PMX, its pyrimidine-binding site is remained. This preserved pyrimidine-binding site would explain the high TS inhibitory activity of HA-ADH-PMX with the same level as native PMX. It was supposed that pyrimidine moiety might bind to the

enzyme much stronger than glutamate moiety. To the best of our knowledge, this would be the first report on measuring TS inhibitory activity of antifolate-polymer conjugates via cell-free assay.

Figure 4B also shows the time course of the absorbance change during the incubation with DHFR. The activities of DHFR in the presence of HA-ADH-PMX (76 kDa) and HA-ADH-PMX (130 kDa) were significantly lower than control group, suggesting that HA-ADH-PMXs retained DHFR inhibitory activities after the conjugation; the absorbance change for HA-ADH-PMX (76 kDa) and HA-ADH-PMX (130 kDa) was 55 % and 47 % of control, respectively. However, their efficacies were almost 5 times less than that of native PMX. According to the previous report (Hanauske, et al., 2001), inhibitory activity of native PMX against DHFR is almost 15 times higher than that against TS. Therefore, investigating the inhibitory effect of HA-ADH-PMXs against DHFR is quite important for the evaluation of their therapeutic effect. Thus, further experiments were conducted to obtain the inhibition constant of HA-ADH-PMXs.

Figure 4C shows the plot of initial velocity of the absorbance change as a function of DHF concentration, which was converted to the double-reciprocal plots (Figure 4D) to determine the apparent Michaelis constant (K_M') and inhibition constant (K_I). As shown in Figure 4D, all plots had almost same value of y-intercept regardless of the existence of inhibitors, which was a characteristic of competitive inhibition. The obtained constants

were summarized in Table 2. Although all PMX derivatives indicated DHFR inhibition, K_I of native PMX was 30 times and 8.3 times higher than that of HA-ADH-PMX (76 kDa) and HA-ADH-PMX (130 kDa). To the best of our knowledge, this is the first report that evaluated the inhibitory activity of PMX conjugates against DHFR via cell-free assay, although that of MTX conjugates has been already reported. In previous reports, MTX conjugated with, e. g., dendrimer (Gurdag, et al., 2006; Li, et al., 2012) and PEG (Riebeseel, et al., 2002) showed inhibitory activity against DHFR, yet their activities were less than native MTX, which was consistent with the case of HA-ADH-PMX. It has been reported that PMX binds to DHFR with its 2-amino group and N3 of the pteridine ring (Abali, et al., 2008; Singh, et al., 2018), both of which were preserved in HA-ADH-PMXs. Therefore, the decrease in the inhibitory activity would be explained by e.g., mobility of the binding moieties. In addition, it was also found that HA-ADH-PMX (130 kDa) could inhibit DHFR more effectively than HA-ADH-PMX (76 kDa). The above inhibitory examinations demonstrated that HA-ADH-PMX had the inhibit activity of folate metabolic enzymes even after the PMX conjugation to HA.

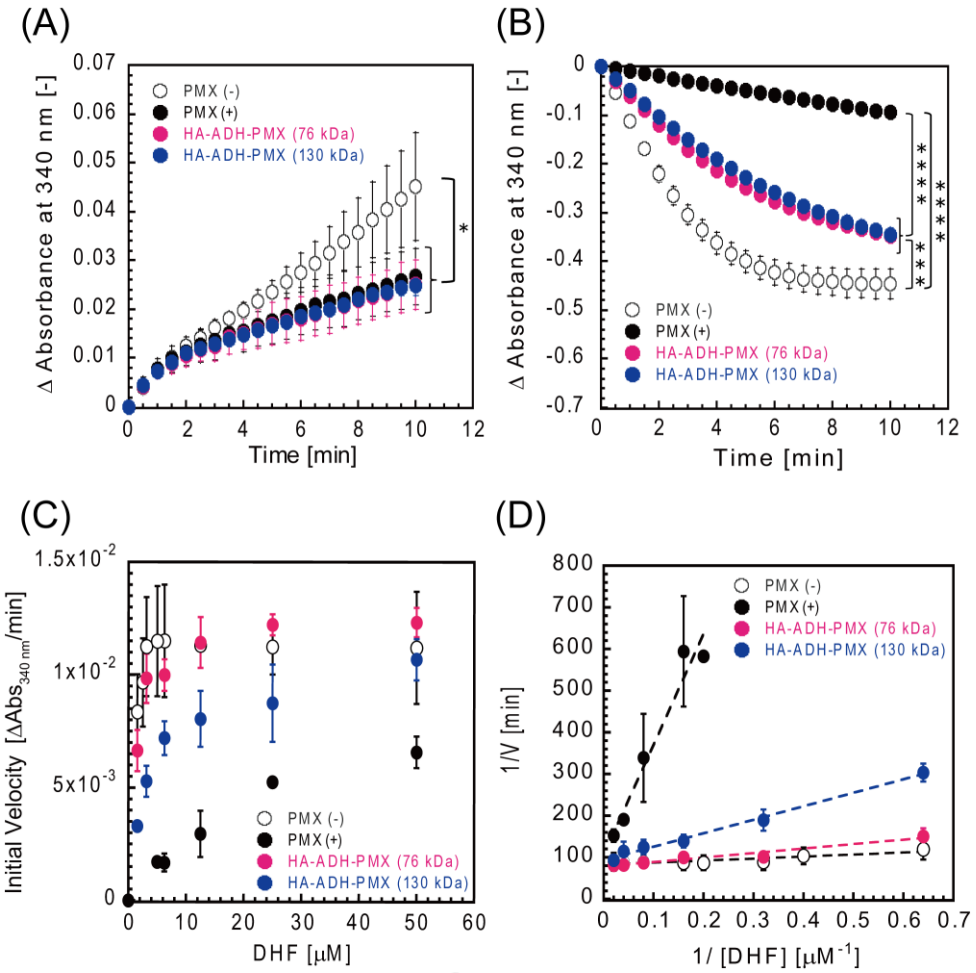

FIGURE 4. INHIBITION OF (A) TS AND (B) DHFR ACTIVITY BY HA-ADH-PMX. TIME COURSE OF THE ABSORBANCE AT 340 NM WITH THE EXISTENCE OF PMX OR HA-ADH-PMX IS SHOWN. (C) PLOT OF INITIAL VELOCITY VERSUS DHF CONCENTRATION FOR DHFR CATALYZED REACTION. (D) RECIPROCAL PLOT OF INITIAL VELOCITY VERSUS DHF CONCENTRATION FOR DHFR CATALYZED REACTION. (PH =7.5, AT 37 °C) STATISTICAL SIGNIFICANCE IS DETERMINED AT $P < 0.05$*, $P < 0.001$***, $P < 0.0001$**** BY ANOVA (N = 3).

Table 2. Determined V_{max}, K_m, K_M' and K_i from DHFR inhibition assay (pH =7.5, at 37 °C)

	V_{max} [min^{-1}]	K_m [μM]	K_M' [μM]	K_i [μM]
PMX (-)	1.2×10^{-2}	0.58	—	—

PMX	9.4×10^{-3}	—	25	2.4×10^{-2}
HA-ADH-PMX (76 kDa)	1.3×10^{-2}	—	1.4	0.73
HA-ADH-PMX (130 kDa)	1.1×10^{-2}	—	3.5	0.20

3.3. Dependency of cellular uptake of HA-ADH-PMX on molecular weight

Rhodamine conjugated HA-ADH-PMXs were synthesized for evaluating the amount of cellular uptake. The reaction scheme and their fluorescent spectra are shown in Figure S1. As shown in Figure 5A, cellular uptake of rhodamine conjugated HA-ADH-PMX was examined after 6 h of exposure by fluorescent microscopy using MPM cell lines (MSTO-211H and AB22) and a mesothelial cell line (MeT-5A). HA-ADH-PMXs with both molecular weights were confirmed to be internalized into all cell lines within 6 h. They were localized in dotted pattern, suggesting their internalization via endocytosis. CD44 mediated endocytosis through the interaction with HA, as well as FRα-mediated endocytosis via interaction with PMX (Wibowo, et al., 2013) would be possible internalization pathways. In addition, comparing between different molecular weights, HA-ADH-PMX (76 kDa) showed higher cellular uptake than HA-ADH-PMX (130 kDa). The amount of cellular uptake was further analyzed quantitatively by flow cytometry (Figure 5B). The cellular uptake amount of HA-ADH-PMX (76 kDa) was significantly higher than HA-ADH-PMX (130 kDa) for all cell lines, which was a

SAME TREND WITH THE FLUORESCENT MICROSCOPIC OBSERVATIONS. THE HIGHER UPTAKE OF HA-ADH-PMX (76 KDA) IS PRESUMABLY DUE TO ITS less polymer entanglement or low molecular size (Table 1).

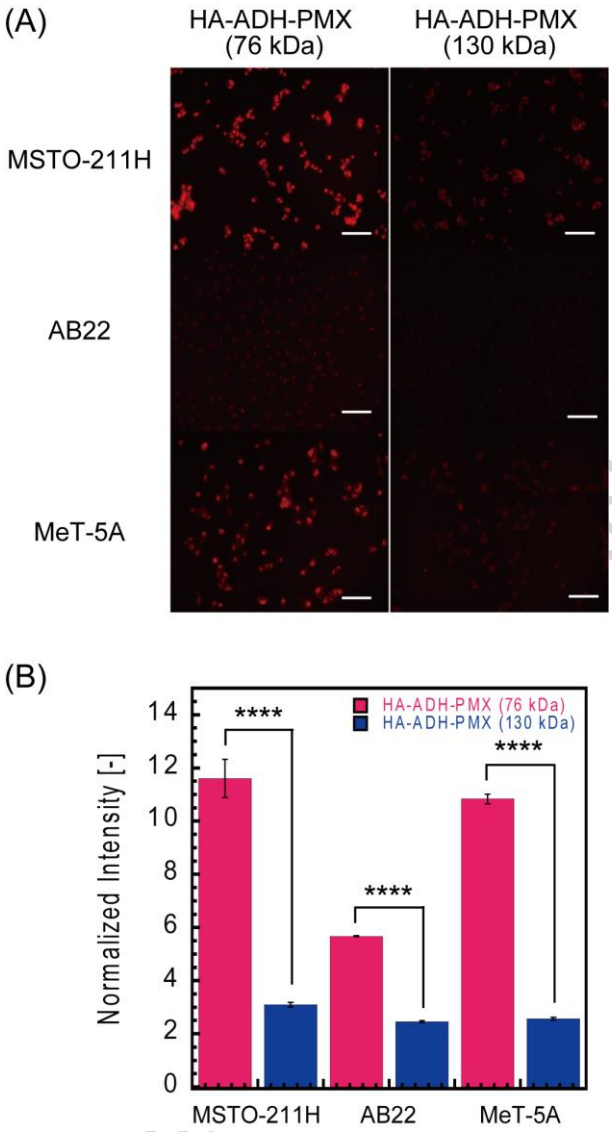

FIGURE 5. CELLULAR UPTAKE OF RHODAMINE LABELED HA-ADH-PMX IN DIFFERENT CELL LINES AS DETECTED THROUGH (A) FLUORESCENT MICROSCOPY AND (B) FLOW CYTOMETRY AFTER 6 H OF INCUBATION. SCALE BAR = 100 µM. STATISTICAL SIGNIFICANCE IS DETERMINED AT $P < 0.0001$**** BY STUDENT'S T-TEST. (N=3)

3.4. Preservation but decrease of anti-tumor activity of HA-ADH-PMXs compared to native PMX in different MPM cell lines

Cytotoxicity of HA-ADH-PMX was evaluated via WST-8 assay using MPM cell lines (MSTO-211H and AB22) and a mesothelial cell line (MeT-5A). Figure 6 shows the cell viabilities plotted as a function of PMX concentration 48 h after the treatment with PMX and HA-ADH-PMXs. Both molecular weight of HA-ADH-PMXs showed dose dependent cytotoxicity in all cell lines. Cytotoxic effect was native PMX > HA-ADH-PMX (130 kDa) > HA-ADH-PMX (76 kDa). These results suggested that cell cytotoxicity was dependent on the molecular weight of HA-ADH-PMX. In addition, compared with native PMX, the cytotoxic effects of HA-ADH-PMX significantly decreased.

To clarify the kinetics of the cytotoxic effect of HA-ADH-PMXs, we also examined the cell viability as a function of exposure time of PMX and HA-ADH-PMXs in MSTO-211H and AB22 cells (Figure 7). After 1, 3, 6, 10 h of PMX exposure, the cells were washed with PBS, followed by the addition of fresh culture media. The cells were incubated for another 24 h and the cell viability was evaluated via WST-8 assay. We used 10 μg/mL of PMX, which showed high cytotoxicity for all reagents after 48h in Figure 6, so that we could focus on the time dependency of cytotoxicity. Cell viability was decreased depending on the exposure time of PMX and HA-ADH-PMX. Native PMX showed high cytotoxicity with shortest exposure time among these reagents. HA-ADH-PMX (130 kDa) showed lower toxicity than native PMX when exposure time was

INSUFFICIENT, THEN REACHED AT THE SAME LEVEL WITHIN 6 H. FURTHERMORE, HA-ADH-PMX (76 KDA) DID NOT SHOW ANY TOXICITY WITHIN 10 H OF EXPOSURE, ALTHOUGH IT REACHES TO SAME LEVEL AFTER 48H AS SHOWN IN FIGURE 6. THESE DELAYS FOR THE CYTOTOXIC ACTIVITY OF HA-ADH-PMX WOULD BE EXPLAINED BY THEIR INTERNALIZATION VIA ENDOCYTOSIS, WHICH GENERALLY TAKES LONGER TIME COMPARED WITH THE UPTAKE OF SMALL MOLECULAR DRUGS VIA TRANSPORTERS (WIBOWO, ET AL., 2013; ZHAO, ET AL., 2014).

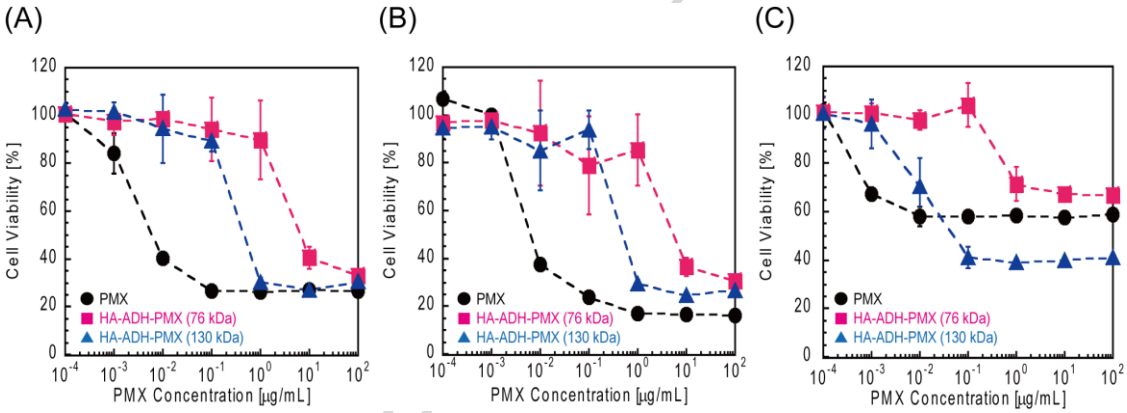

FIGURE 6. CELL VIABILITY OF (A) MSTO-211H, (B) AB22 AND (C) MET-5A INCUBATED WITH HA-ADH-PMX POLYMERS OR FREE PMX FOR 48 H. (N = 3)

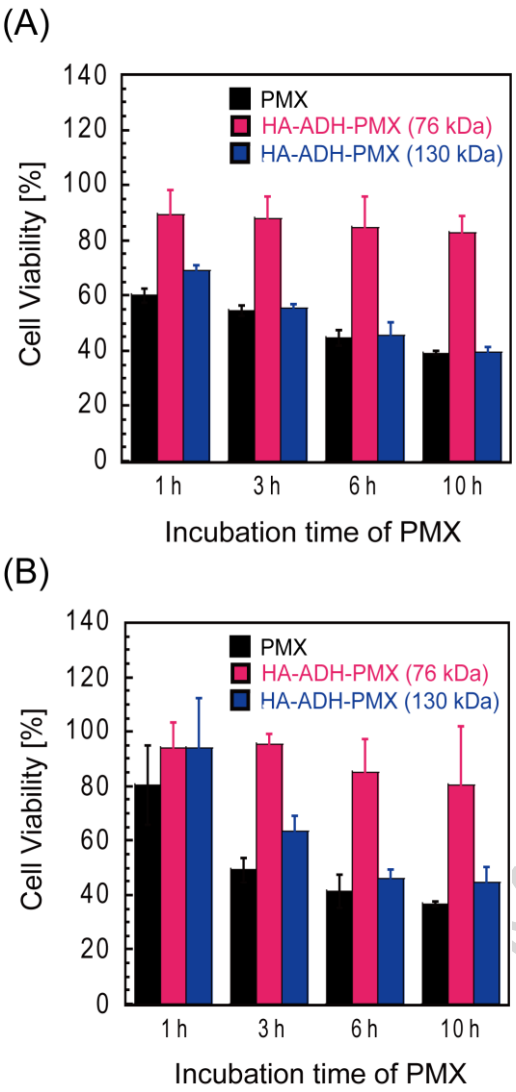

FIGURE 7. CELL VIABILITY OF (A) MSTO-211H AND (B) AB22 TREATED WITH HA-ADH-PMX POLYMERS OR FREE PMX AT DIFFERENT INCUBATION TIME. CELL VIABILITY WAS MEASURED 24H AFTER THE START OF THE TREATMENT. PMX CONCENTRATION WAS 10 μG/ML. (N = 4)

3.5. EVALUATION OF ANTITUMOR ACTIVITY IN MOUSE MODELS OF MALIGNANT PLEURAL MESOTHELIOMA (MPM)

The antitumor effect of HA-ADH-PMX was evaluated against MPM mouse model using AB22 cells. Seven days after AB22 cells inoculation in pleural cavity, PMX and HA-ADH-PMXs were injected intrapleurally. The survival time of mice were

recorded until all mice died. Median survival times were 39, 40, 50 and 52 days in HA-ADH-PMX (130 kDa), control without material injections, HA-ADH-PMX (76 kDa), and native PMX group, respectively. The weight changes of mice were shown in Table S1 in supplementary information. Survival time of HA-ADH-PMX (130 kDa) group was comparable with that of control. On the other hand, despite of the lower *in vitro* cytotoxicity than HA-ADH-PMX (130 kDa), the average survival time of HA-ADH-PMX (76 kDa) group was longer than control, and almost the same with that of native PMX group, although there was no significant difference.

In the clinical standard regimen, PMX is first administered intravenously at 500 mg/m^2, followed by the intravenous administration of cisplatin at 75 mg/m^2 on day 1 of each 21-day cycle. Following this clinical standard protocol, many researches administered 10 mg/kg of PMX, either intravenously or intrapleurally, once every 3 days for 2-6 times in animal experiments (ANDO, ET AL., 2015; ELDIN, ET AL., 2016; LU, ET AL., 2016). On the other hand, in this research, we administered 60 mg/kg of PMX in a single shot, assuming endoscopic administration of materials into pleural cavity due to the several advantages of intrapleural chemotherapy (HAAS AND STERMAN, 2012). Furthermore, it was expected that HA-ADH-PMX could retain in pleural cavity because of its high viscoelasticity. Although our results showed no significant difference among all groups, there is a possibility that therapeutic effect of HA-ADH-PMX will be increased by multiple administrations in the same way as previous researches.

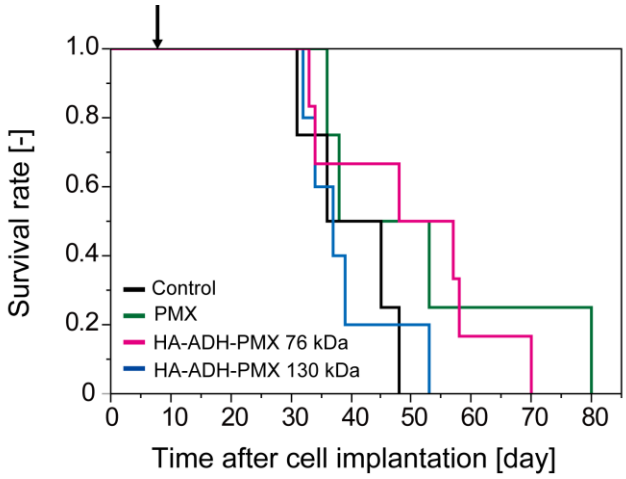

FIGURE 8. SURVIVAL CURVES OF MPM MODEL MICE TREATED WITH HA-ADH-PMX OR FREE PMX. RESULT OF MPM MODEL MICE WITHOUT ANY TREATMENT IS ALSO SHOWN AS CONTROL. ARROW INDICATES A TIME POINT WHERE PMX WAS INJECTED. MICE WERE TREATED AS FOLLOWS: UNTREATED (N = 4); PMX (N = 4); HA-ADH-PMX 76 KDA (N = 6); HA-ADH-PMX 130 KDA (N = 5).

3.6. RELATIONSHIP BETWEEN ANTI-TUMOR EFFECTS AND MOLECULAR WEIGHT OF HA-ADH-PMXS

IN THIS STUDY, PMX-CONJUGATED HAS OF DIFFERENT MOLECULAR WEIGHT WERE SYNTHESIZED FOR THE FIRST TIME. OUR RESULTS REVEALED THAT HA-ADH-PMX SHOWED INTERESTING MOLECULAR WEIGHT-DEPENDENT ACTIVITIES. WHILE HA-ADH-PMX (130 kDa) had higher cytotoxicity than HA-ADH-PMX (76 kDa) *in vitro* (Figures 6-7), the *in vivo* antitumor effect of HA-ADH-PMX (76 kDa) was higher than that of HA-ADH-PMX (130 kDa) (Figure 8). This different tendency between *in vitro* and *in vivo* would be explained by the combined effect of the transport kinetics and enzyme inhibitory activity. Whereas HA-ADH-PMX (76 kDa) showed higher cellular uptake (Figure 5), inhibitory activity against FOLATE METABOLIC enzymes was higher in HA-ADH-PMX (130 kDa)

(Figure 4). We consider that since the difference in the enzyme inhibitory activity was more dominant, HA-ADH-PMX (130 kDa) showed higher cytotoxicity *in vitro*. On the other hand, in the case of *in vivo*, transport kinetics of HA-ADH-PMX would be involved. For example, MPM model of AB22 cells produces highly viscous pleural effusion containing blood in the pleural cavity (Figure S4), which would prevent the penetration of HA-ADH-PMX (130 kDa).

It has been known that molecular weight of polymer-drug conjugates affects their therapeutic effect. In the case of antifolates, conjugation of MTX to PEG (750 Da-40 kDa) (Riebeseel, et al., 2002) or dextran (10 kDa-500 kDa) (Nevozhay, et al., 2006) with various molecular weight have been reported. *In vitro* cytotoxicity of both MTX-polymer conjugates was lower than native MTX and decreased with increasing molecular weight. On the other hand, both conjugates showed significant *in vivo* therapeutic effect even with high molecular weight, which would be due to prolonged residence time. These inconsistencies between *in vitro* and *in vivo* results was similar with our case.

Note that an interesting difference between our results and these previous researches (Riebeseel, et al., 2002; Nevozhay, et al., 2006) is that higher molecular weight of HA-ADH-PMX showed higher enzyme inhibitory activity and *in vitro* cytotoxicity. A possible reason is the density of PMX conjugated to HA. The density of PMX in the conjugate was estimated to be 4.3×10^{-3} nm^{-3} for HA-ADH-PMX (76 kDa) and 2.1×10^{-3} nm^{-3} for HA-ADH-PMX (130 kDa) using the characterization results in Table 1, assuming that each

HA-ADH-PMX shows spherical conformation without association with other polymers. The lower PMX density in HA-ADH-PMX (130 kDa) might enhance its interaction with enzymes due to its lower steric hinderance. We evaluated the potential of HA-ADH-PMX for the treatment of MPM in terms of molecular weight of HA-ADH-PMX, the further detailed research about other factors such as modification degree with PMX in necessary. Furthermore, therapeutic target of HA-ADH-PMX is not limited to MPM, and thus is also expected to be applied for non-small cell lung cancer, to which the treatment with PMX is approved.

4. Conclusion

We developed different molecular weight of HA-based PMX conjugates and evaluate their therapeutic activity for MPM. HA-ADH-PMXs retained TS and DHFR inhibitory activities even after conjugation. In particular, its TS inhibitory activity was as high as that of native PMX, and HA-ADH-PMXs were internalization into MPM cells via endocytosis. Although single administration of HA-ADH-PMXs did not show the therapeutic effect as well as free PMX in mice MPM model, dependency of *in vitro* cytotoxicity of HA-ADH-PMXs on their molecular weight showed that their anti-cancer function appeared on the balance between endocytosis and enzyme inhabitation effect, suggesting that molecular weight of HA and modification degree with PMX of HA-ADH-PMX sensitively change the cytotoxicity of HA-ADH-PMXs *in vitro* and *in vivo*.

Acknowledgements

Hyaluronan was kindly gifted by Denka Co. We are grateful to Keyence for the use
of the fluorescence microscope, BZ-X810. This research is supported by The Translational Research program; Strategic Promotion for practical application of Inovative medical Technology, TR-SPRINT (A92), from Japan Agency for Medical Research and Development, AMED.

Conflict of interest

The authors declare no conflicts of interest.

References

Abali, E. E., Skacel, N. E., Celikkaya, H., Hsieh Y. C., 2008. Regulation of human dihydrofolate reductase activity and expression. Vitam. Horm. 79, 267-292.

Ando, H., Kobayashi, S., Abu Lila, A. S., Eldin, N. E., Kato, C., Shimizu, T., Ukawa, M., Kawazoe, K., Ishida, T., 2015. Advanced therapeutic approach for the treatment of malignant pleural mesothelioma via the intrapleural administration of liposomal pemetrexed. J. Controlled Release. 220, Pt A, 29-36.

Baas, P. 2007. Optimising survival in malignant mesothelioma. Lung Cancer. 57, Suppl 2, S24-29.

Boratyński, J., Opolski, A., Wietrzyk, J., Górski, A., Radzikowski, C., 2000. Cytotoxic and antitumor effect of fibrinogen-methotrexate conjugate. Cancer Lett. 148, 2, 189-195.

Bulpitt, P., Aeschlimann, D., 1999. New strategy for chemical modification of hyaluronic acid: preparation of functionalized derivatives and their use in the formation of novel biocompatible hydrogels. J. Biomed. Mater. Res. 47, 2, 152-169.

Cai, S., Thati, S., Bagby, T. R., Diab, H. M., Davies, N. M., Cohen, M. S., Forrest, M. L., 2010. Localized doxorubicin chemotherapy with a biopolymeric nanocarrier improves survival and reduces toxicity in xenografts of human breast cancer. J. Controlled Release 146, 212-218.

Chau, Y., Tan, F.E., Langer, R., 2004. Synthesis and characterization of dextran-peptide-methotrexate conjugates for tumor targeting via mediation by matrix metalloproteinase II and matrix metalloproteinase IX. Bioconjug. Chem. 15, 4, 931-941.

Cichy, J., Pure, E., 2003. The liberation of CD44. J. Cell Biol., 161, 839-843.

Ciekot, J., Goszczyński, T. M., Boratyński, J., 2016. Methods for preliminary determination of pemetrexed in macromolecular drug-carrier systems. Acta Pharm. 66, 1, 147-153.

CREANEY, J., DICK, I. M., SEGAL, A., MUSK, A. W., ROBINSON, B. W., 2013. PLEURAL EFFUSION HYALURONIC ACID AS A PROGNOSTIC MARKER IN PLEURAL MALIGNANT MESOTHELIOMA. LUNG CANCER. 82, 3, 491-498.

EL-NAGGAR, A. M., ABOU-EL-REGAL, M. M., EL-METWALLY, S. A., SHERBINY, F. F., EISSA, I. H., 2017. SYNTHESIS, CHARACTERIZATION AND MOLECULAR DOCKING STUDIES OF THIOURACIL DERIVATIVES AS POTENT THYMIDYLATE SYNTHASE INHIBITORS AND POTENTIAL ANTICANCER AGENTS. MOL. DIVERS. 21, 4, 967-983.

ELDIN, N. E., ABU LILA, A. S., KAWAZOE, K., ELNAHAS, H. M., MAHDY, M. A., ISHIDA, T., 2016. ENCAPSULATION IN A RAPID-RELEASE LIPOSOMAL FORMULATION ENHANCES THE ANTI-TUMOR EFFICACY OF PEMETREXED IN A MURINE SOLID MESOTHELIOMA-XENOGRAFT MODEL. EUR. J. PHARM. SCI. 81, 60-66.

EMOTO, S., YAMAGUCHI, H., KAMEI, T., ISHIGAMI, H., SUHARA, T., SUZUKI, Y., ITO, T., KITAYAMA, J., WATANABE, T., 2014. INTRAPERITONEAL ADMINISTRATION OF CISPLATIN VIA AN IN SITU CROSS-LINKABLE HYALURONIC ACID-BASED HYDROGEL FOR PERITONEAL DISSEMINATION OF GASTRIC CANCER. SURG. TODAY 44, 5, 919-926.

FUJIMOTO, N., AOE, K., KOZUKI, T., OZE, I., KATO, K., KISHIMOTO, T., HOTTA, K., 2018. A PHASE II TRIAL OF FIRST-LINE COMBINATION CHEMOTHERAPY WITH CISPLATIN, PEMETREXED, AND NIVOLUMAB FOR UNRESECTABLE

MALIGNANT PLEURAL MESOTHELIOMA: A STUDY PROTOCOL. CLIN. LUNG CANCER. 19, 5, E705-E707

GENOVA, C., RIJAVEC, E., TRUINI, A., COCO, S., SINI, C., BARLETTA, G., DAL BELLO, M. G., ALAMA, A., SAVARINO, G., PRONZATO, P., BOCCARDO, F., GROSSI F., 2013. PEMETREXED FOR THE TREATMENT OF NON-SMALL CELL LUNG CANCER. EXPERT OPIN. PHARMACOTHER. 14, 11, 1545-1558.

GURDAG, S., KHANDARE, J., STAPELS, S., MATHERLY, L. H., KANNAN, R. M., 2006. ACTIVITY OF DENDRIMER-METHOTREXATE CONJUGATES ON METHOTREXATE-SENSITIVE AND -RESISTANT CELL LINES. BIOCONJUG. CHEM. 17, 2, 275-283.

HAAS, A. R., STERMAN, D. H., 2012. NOVEL INTRAPLEURAL THERAPIES FOR MALIGNANT DISEASES. RESPIRATION. 83, 4, 277-292.

HANAUSKE, A. R., CHEN, V., PAOLETTI, P., NIYIKIZA, C., 2001. PEMETREXED DISODIUM: A NOVEL ANTIFOLATE CLINICALLY ACTIVE AGAINST MULTIPLE SOLID TUMORS. ONCOLOGIST. 6, 4, 363-373.

HARDING, S. E., 1997. THE INTRINSIC VISCOSITY OF BIOLOGICAL MACROMOLECULES. PROGRESS IN MEASUREMENT, INTERPRETATION AND APPLICATION TO STRUCTURE IN DILUTE SOLUTION. PROG. BIOPHYS. MOL. BIOL. 68, 2-3, 207-262.

HOMMA, A., SATO, H., OKAMACHI, A., EMURA, T., ISHIZAWA, T., KATO, T., MATSUURA, T., SATO, S., TAMURA, T., HIGUCHI, Y., WATANABE, T., KITAMURA, H., ASANUMA, K., YAMAZAKI, T., IKEMI, M., KITAGAWA, H., MORIKAWA, T., IKEYA, H., MAEDA, K., TAKAHASHI, K., NOHMI, K., IZUTANI, N., KANDA, M., SUZUKI, R., 2009. NOVEL HYALURONIC ACID-METHOTREXATE CONJUGATES FOR OSTEOARTHRITIS TREATMENT. BIOORG. MED. CHEM. 17, 13, 4647-4656.

KAO, T. T., WANG, K. C., CHANG, W. N., LIN, C. Y., CHEN, B. H., WU, H. L., SHI, G. Y., TSAI, J. N., FU, T. F., 2008. CHARACTERIZATION AND COMPARATIVE STUDIES OF ZEBRAFISH AND HUMAN RECOMBINANT DIHYDROFOLATE REDUCTASES--INHIBITION BY FOLIC ACID AND POLYPHENOLS. DRUG METAB. DISPOS. 36, 508-516.

LEE, H., LEE, K., PARK, T. G., 2008. HYALURONIC ACID-PACLITAXEL CONJUGATE MICELLES: SYNTHESIS, CHARACTERIZATION, AND ANTITUMOR ACTIVITY. BIOCONJUG. CHEM. 19, 6, 1319-1325.

LI, M. H., CHOI, S. K., THOMAS, T. P., DESAI, A., LEE, K. H., KOTLYAR, A., BANASZAK HOLL M. M., BAKER, J. R. JR., 2012. DENDRIMER-BASED MULTIVALENT METHOTREXATES AS DUAL ACTING NANOCONJUGATES FOR CANCER CELL TARGETING. EUR. J. MED. CHEM. 47, 1, 560-572.

LI, Y., HELDIN, P., 2001. HYALURONAN PRODUCTION INCREASES THE MALIGNANT PROPERTIES OF MESOTHELIOMA CELLS. BR. J. CANCER. 85, 4, 600-607.

LOURDES, C-D., RALPH, A. S., 2017. CD44 AND ITS LIGAND HYALURONAN AS POTENTIAL BIOMARKERS IN MALIGNANT PLEURAL MESOTHELIOMA: EVIDENCE AND PERSPECTIVES. RESPIR. RES. 18, 58.

LU, N., LI, R., LIU, Q., HU, B., XU, X., JI, C., HAN, X., WANG, P., LIU, B., 2016. ANTITUMOR AND ANTIMETASTATIC EFFECTS OF PEMETREXED-LOADED TARGETED NANOPARTICLES IN B16 BEARING MICE. DRUG DELIV. 23, 7, 2566-2574.

LUO, Y., BERNSHAW, N. J., LU, Z.-R., KOPECEK, J., PRESTWICH, G. D., 2002. TARGETED DELIVERY OF DOXORUBICIN BY HPMA COPOLYMERHYALURONAN BIOCONJUGATES. PHARM. RES. 19, 396-402.

LUO, Y., PRESTWICH, G. D., 1999. SYNTHESIS AND SELECTIVE CYTOTOXICITY OF A HYALURONIC ACID-ANTITUMOR BIOCONJUGATE. BIOCONJUG. CHEM. 10, 5, 755-763.

MISRA, S., HASCAL,L V. C., MARKWALD, R. R., GHATAK, S., 2015. INTERACTIONS BETWEEN HYALURONAN AND ITS RECEPTORS (CD44, RHAMM) REGULATE THE ACTIVITIES OF INFLAMMATION AND CANCER. FRONT IMMUNOL. 6, 6, 201.

NAVARRO-PERÁN, E., CABEZAS-HERRERA, J., HINER, A. N., SADUNISHVILI, T., GARCÍA-CÁNOVAS, F., RODRÍGUEZ-LÓPEZ, J. N., 2005. KINETICS OF THE INHIBITION OF BOVINE LIVER DIHYDROFOLATE REDUCTASE BY TEA

CATECHINS: ORIGIN OF SLOW-BINDING INHIBITION AND pH STUDIES. BIOCHEMISTRY. 44, 7512-7525.

NEVOZHAY, D., BUDZYNSKA, R., KANSKA, U., JAGIELLO, M., OMAR, M. S., BORATYNSKI, J., OPOLSKI, A., 2006. ANTITUMOR PROPERTIES AND TOXICITY OF DEXTRAN-METHOTREXATE CONJUGATES ARE DEPENDENT ON THE MOLECULAR WEIGHT OF THE CARRIER. ANTICANCER RES. 26, 2A, 1135-1143.

OHTA, S., HIRAMOTO, S., AMANO, Y., EMOTO, S., YAMAGUCHI, H., ISHIGAMI, H., KITAYAMA, J., ITO, T., 2017. INTRAPERITONEAL DELIVERY OF CISPLATIN VIA A HYALURONAN-BASED NANOGEL/IN SITU CROSS-LINKABLE HYDROGEL HYBRID SYSTEM FOR PERITONEAL DISSEMINATION OF GASTRIC CANCER. MOL. PHARM. 14, 9, 3105-3113.

OHTA, S., HIRAMOTO, S., AMANO, Y., SATO, M., SUZUKI, Y., SHINOHARA, M., EMOTO, S., YAMAGUCHI, H., ISHIGAMI, H., SAKAI, Y., KITAYAMA, J., ITO, T., 2016. PRODUCTION OF CISPLATIN-INCORPORATING HYALURONAN NANOGELS VIA CHELATING LIGAND-METAL COORDINATION. BIOCONJUG. CHEM. 27, 3, 504-508.

OOMMEN, O. P., GAROUSI, J., SLOFF, M., VARGHESE, O. P., 2014. TAILORED DOXORUBICIN-HYALURONAN CONJUGATE AS A POTENT ANTICANCER GLYCO-DRUG: AN ALTERNATIVE TO PRODRUG APPROACH. MACROMOL. BIOSCI. 14, 3, 327-333.

PRAVATA, L., BRAUD, C., BOUSTTA, M., EI GHZAOUI, A., TØMMERAAS, K., GUILLAUMIE, F., SCHWACH-ABDELLAOUI, K., VERT M., 2008. NEW AMPHIPHILIC LACTIC ACID OLIGOMER-HYALURONAN CONJUGATES: SYNTHESIS AND PHYSICOCHEMICAL CHARACTERIZATION. BIOMACROMOLECULES 9, 1, 340-348.

RIEBESEEL, K., BIEDERMANN, E., LÖSER, R., BREITER, N., HANSELMANN, R., MÜLHAUPT, R., UNGER, C., KRATZ, F., 2002. POLYETHYLENE GLYCOL CONJUGATES OF METHOTREXATE VARYING IN THEIR MOLECULAR WEIGHT FROM MW 750 TO MW 40000: SYNTHESIS, CHARACTERIZATION, AND STRUCTURE-ACTIVITY RELATIONSHIPS IN VITRO AND IN VIVO. BIOCONJUG. CHEM. 13, 4, 773-785.

SASAI, M., NAKAMURA, H., SOUGAWA, N., SAKURAI, Y., SUZUKI, M., LEE, C. M., 2016. NOVEL HYALURONAN FORMULATION ENHANCES THE EFFICACY OF BORON NEUTRON CAPTURE THERAPY FOR MURINE MESOTHELIOMA. ANTICANCER RES. 3, 907-911.

SCHULTZ, R. M., 2005. PRECLINICAL DEVELOPMENT OF ALIMTA (PEMETREXED, LY231514), A MULTITARGETED ANTIFOLATE. PROG. DRUG RES. 63, 275-300.

SHIN, J. M., KIM, S. H., THAMBI, T., YOU, D. G., JEON, J., LEE, J. O., CHUNG, B. Y., JO, D. G., PARK, J. H., 2014. A HYALURONIC ACID-METHOTREXATE CONJUGATE FOR TARGETED THERAPY OF RHEUMATOID ARTHRITIS. CHEM. COMMUN. 50, 57, 7632-7635.

SINGH, A., DESHPANDE, N., PRAMANIK, N., JHUNJHUNWALA, S., RANGARAJAN, A., ATREYA, H. S., 2018. OPTIMIZED PEPTIDE BASED INHIBITORS TARGETING THE DIHYDROFOLATE REDUCTASE PATHWAY IN CANCER. SCI. REP. 8, 3190.

STONE, S. R., MORRISON, J. F., 1986. MECHANISM OF INHIBITION OF DIHYDROFOLATE REDUCTASES FROM BACTERIAL AND VERTEBRATE SOURCES BY VARIOUS CLASSES OF FOLATE ANALOGUES. BIOCHIM. BIOPHYS. ACTA. 869, 275-285.

THOMPSON, J. K., WESTBOM, C. M., SHUKLA, A., 2014. MALIGNANT MESOTHELIOMA: DEVELOPMENT TO THERAPY. J. CELL BIOCHEM. 115, 1, 1-7.

VANDANA, M., SAHOO, S. K., 2012. REDUCED FOLATE CARRIER INDEPENDENT INTERNALIZATION OF PEGYLATED PEMETREXED: A POTENTIAL NANOMEDICINAL APPRORCH FOR BREAST CANCER THERAPY. MOL. PHARM. 9, 10, 2828-2843.

WAHBA, A. J., FRIEDKIN, M., 1962. THE ENZYMATIC SYNTHESIS OF THYMIDYLATE. I. EARLY STEPS IN THE PURIFICATION OF THYMIDYLATE SYNTHETASE OF ESCHERICHIA COLI. J. BIOL. CHEM. 237, 3794-3801.

WEIGEL, P. H., BAGGENSTOSS, B. A., 2017. WHAT IS SPECIAL ABOUT 200 KDA HYALURONAN THAT ACTIVATES HYALURONAN RECEPTOR SIGNALING? GLYCOBIOLOGY. 27, 9, 868-877.

WIBOWO, A. S., SINGH, M., REEDER, K. M., CARTER, J. J., KOVACH, A. R., MENG, W., RATNAM, M., ZHANG, F., DANN, C. E. 3RD., 2013. STRUCTURES OF HUMAN FOLATE RECEPTORS REVEAL BIOLOGICAL TRAFFICKING STATES AND DIVERSITY IN FOLATE AND ANTIFOLATE RECOGNITION. PNAS 110, 38, 15180-15188.

YEO, Y., HIGHLEY, C. B., BELLAS, E., ITO, T., MARINI, R., LANGER, R., KOHANE, D. S., 2006. IN SITU CROSS-LINKABLE HYALURONIC ACID HYDROGELS PREVENT POST-OPERATIVE ABDOMINAL ADHESIONS IN A RABBIT MODEL. BIOMATERIALS 27, 27, 4698-4705.

ZHAO, R., DIOP-BOVE, N., GOLDMAN, I. D., 2014. ENHANCED RECEPTOR-MEDIATED ENDOCYTOSIS AND CYTOTOXICITY OF A FOLIC ACID-DESACETYLVINBLASTINE MONOHYDRAZIDE CONJUGATE IN A PEMETREXED-RESISTANT CELL LINE LACKING FOLATE-SPECIFIC FACILITATIVE CARRIERS BUT WITH INCREASED FOLATE RECEPTOR EXPRESSION. MOL. PHARMACOL. 85, 2, 310-321.

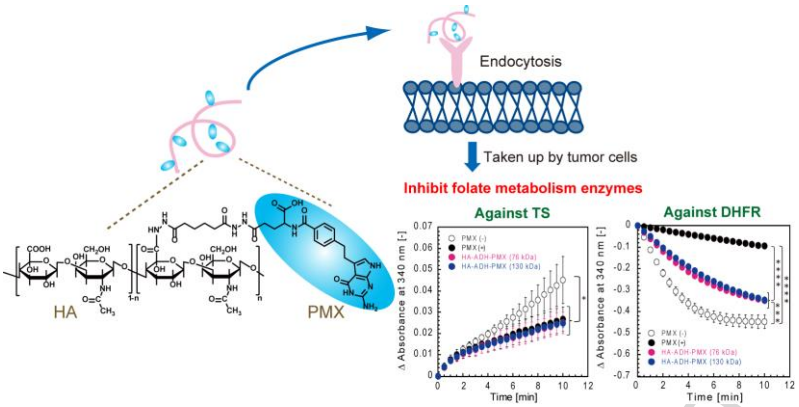

Graphical abstract